Deliverable D1.1

Current methodology for temperature measurements in industrial linings

Document type	**Deliverable D 1.1**
Document Version / Status	**1.1**
Primary Authors	**Marc Huger, marc.huger@unilim.fr, UNILIM**
Distribution Level	**PU (Public)**
Project Acronym	**ATHOR**
Project Title	**Advanced THermomechanical multiscale mOdelling of Refractory linings**
Grant Agreement Number	**764987**
Project Website	**www.etn-athor.eu**
Project Coordinator	**Marc Huger, marc.huger@unilim.fr, UNILIM**
Document Contributors	**Marc Huger, marc.huger@unilim.fr, UNILIM** **Diana Vitiello, diana.vitiello@unilim.fr, UNILIM** **Rafael Oliveira, rafael.oliveira@uc.pt, UMINHO**

History of Changes

Version	Date	Author (Organization)	Change	Page
1.1	16.07.2019	Diana Vitiello (UNILIM), Rafael Oliveira (UMINHO)	Creation of the first version	all
1.2	31.08.2019	Glyn Derrick (UNILIM)	General formatting, English check	all
1.3	03.09.2019	Diana Vitiello (UNILIM), Rafael Oliveira (UMINHO)	General correction, addition of a conclusion	all

Table 1. Related Work Packages status

Work package		Status	Description
WP 1: Improvement of measurement tools	Task 1.1: thermal instrumentation		Description of three main thermal instrumentation and applications in ATHOR project.

Table of contents

1. Introduction

Task 1.1 “thermal instrumentation” is dedicated to the development of methodologies for temperature measurements up to 1500°C in steel ladle linings. It will be applied on laboratory scale tests (UMINHO, RHI-Magnesita and TATASTEEL) on masonry and for industrial applications like refractory linings in steel ladles (TATASTEEL).

In this report, the thermal equipment used in the ATHOR project and examples of their use are discussed. In Section 2 a description, including the working principle and the main advantages / disadvantages, of three thermal instruments is given. These devices are: thermocouples, infrared camera and laser scanner. In section 3, some examples of the use of this equipment within the ATHOR project are given, both in laboratory scale and in-situ measurements.

2. Thermal instrumentation

The lining of each steel ladle is composed of different materials with specific temperature dependent properties. In other words, the properties of the materials under service conditions are not the same as at room temperature. The acquisition of the temperature data at different points through the steel ladle lining and the effect of this on the properties of the materials used, commonly known as the temperature field, is therefore of paramount importance. Hence, the main goal of this task is to improve the methodologies used for temperature measurements in industrial applications. This ambitious purpose includes the development of laboratory scale equipment as well as industrial in-situ devices.

The thermal instrumentation that will be used and improved are:

- Thermocouples;
- Infrared (IR) camera;
- Laser scanner.

2.1. Thermocouples

A thermocouple is an electrical device for temperature measurement, which generates a voltage that changes with temperature[1]. It is comprised of at least two metals joined together to form two junctions: one is connected to the body which will have its temperature measured (this is the hot or measuring junction); the other is connected to a body of known temperature (this is the cold or reference junction). As the temperature changes from the junction to the ends of the wires, a voltage develops across the junction. Figure 1 shows a scheme of the thermocouple circuit.

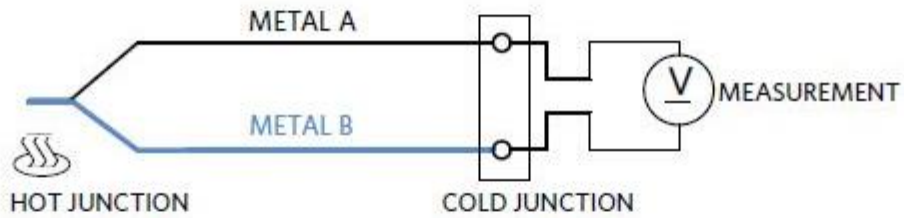

Figure 1: Scheme of a thermocouple circuit.

If the temperature at the two junctions is the same, there is no flow of current through the thermocouple because equal and opposite electromotive forces (emf) are generated simultaneously. While if the two junctions are at different temperatures, the emf cannot be equal to zero and a net current flows through the circuit. The magnitude of this force depends on the materials used in the device. The amount of emf developed within the thermocouple circuit is very small, usually in millivolts, therefore highly sensitive instruments are required to carry out the measurement. Two commonly used devices are; the ordinary galvanometer and voltage balancing potentiometer.

The working principle is based on three effects, discovered by Seebeck, Peltier and Thomson:

- <u>*Seebeck effect*</u>: when a metal bar is heated at one end, a voltage (known as the Seebeck voltage) develops across the length of the bar. This voltage changes with the temperature and the type of metal used. By joining dissimilar metals that have different Seebeck voltages at a temperature-sensing junction, a thermocouple voltage (VTC) is generated.
- <u>*Peltier effect*</u>: it is the reverse phenomenon of the Seebeck effect; when a potential difference is applied across a thermocouple, it causes a temperature difference between the junctions of the different materials in the thermocouple. As a result of this effect, an electronic refrigerator can be made, which is known as the Peltier cooler.

European Commission
Horizon 2020
European Union funding
for Research & Innovation

- *Thomson effect:* the evolution or absorption of heat when an electrical current passes through a circuit composed of a single material that has a temperature difference along its length. This transfer of heat is superimposed on the common production of heat associated with the electrical resistance to currents in conductors.

Combinations of different metals create a variety of voltage responses. This leads to different types of thermocouples used for different temperature ranges and accuracies (Table 1). The choice depends on: the temperature range required for the experiment, temperature accuracy, durability, conditions of use, expected service life, price etc.

Table 1: List of different available thermocouples. The most common and used is the type K.

Type	Material	Temperature Range	Accuracy
Type B	Platinum Rhodium - 30% / Platinum Rhodium - 6%	200ºC to 1700ºC	+/- 0.50%
Type S	Platinum Rhodium - 10% / Platinum	-50ºC to 1480ºC	+/- 1.5C or +/- 0.25%
Type R	Platinum Rhodium - 13% / Platinum	-50ºC to 1480ºC	+/- 1.5C or +/- 0.25%
Type K	Nickel-Chromium / Nickel-Alumel	-270 ºC to 1260 ºC	+/- 2.2C or +/- 0.75%
Type E	Nickel-Chromium / Constantan	-270ºC to 870ºC	+/- 1.7C or +/- 0.50%
Type J	Iron / Constantan	-210ºC to 760ºC	+/- 2.2C or +/- 0.75%

The thermocouples can be classified into two different construction types: base metal thermocouples and noble metal thermocouples. The first are the most common thermocouples. The second are composed of precious metals such as platinum and rhodium. They are more expensive, and are used in higher temperature applications. The advantages and disadvantages of using thermocouples are summarized in Table 2.

Table 2: Summary of the main advantages and disadvantages of using thermocouples.

Advantages	Disadvantages
Most practical temperature ranges, from cryogenics to jet-engine exhaust, can be served using thermocouples. Depending on the metal wires used, a thermocouple is capable of measuring temperature in the range -200°C to +2500°C.	Substantial signal conditioning is necessary to convert the thermocouple voltage into a usable temperature reading. Traditionally, signal conditioning has required a large investment in design time to avoid introducing errors that degrade accuracy.
Thermocouples are rugged devices that are immune to shock and vibration and are suitable for use in hazardous environments.	In addition to the inherent inaccuracies in thermocouples due to their metallurgical properties, a thermocouple measurement is only as accurate as the reference junction temperature can be measured, traditionally within 1°C to 2°C.
Because they are small and have low thermal capacity, thermocouples respond rapidly to temperature changes, especially if the sensing junction is exposed. They can respond to rapidly changing temperatures within a few hundred milliseconds.	Because thermocouples consist of two dissimilar metals, in some environments, corrosion over time may result in deteriorating accuracy. Hence, they may need protection; and care. Maintenance are thus essential.
Because thermocouples require no excitation power, they are not prone to self heating and are intrinsically safe.	When measuring microvolt-level signal changes, noise from stray electrical and magnetic fields can be a problem. Twisting the thermocouple wire pair can greatly reduce magnetic field pickup. Using a shielded cable or running wires in metal conduit and guarding can reduce electric field pickup. The measuring device should provide signal filtering, either in hardware or by software, with strong rejection of the line frequency (50 Hz/60 Hz) and its harmonics.

European Commission
Horizon 2020
European Union funding
for Research & Innovation

The thermocouples come in several different construction types, as shown in Figure 2. Thermocouples without a protective sheath are known as exposed thermocouples. These are used for small sensors, with direct heat transfer from the measured object. This type of thermocouple gives a fast sensor response. In a grounded thermocouple, the sensor is welded to the sheath. Often this sheath is composed of metal, which also allows for heat transfer, but adds an extra protection for harsh and difficult environments. However, because the thermocouple is welded to the metal sheath, there is an electrical contact. This makes the measurement susceptible to noise from ground loops. A sealed thermocouple is isolated from the sheath, adding a layer of insulation between the thermocouple and the measured object. This type of thermocouple has the slowest temperature response because of the insulating layer.

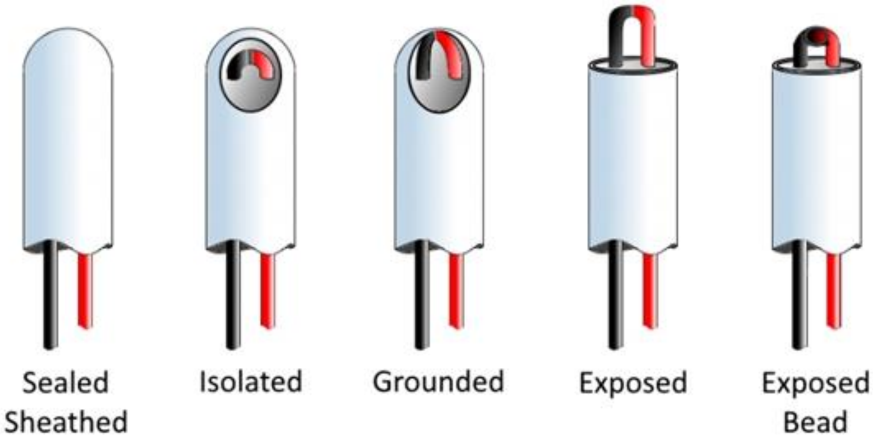

Figure 2: Thermocouple Construction Types.

2.2. Infrared (IR) camera

The infrared camera or thermal camera is an innovative tool that can measure the temperature distribution on the external surface of the steel ladle while the overhead crane transports it. This allows the continuous production of steel without contact between the camera and the analysed object. For covering the complete outer surface of the ladle including the bottom, generally 4 - 5 cameras are required. It should be noted that the IR camera cannot see through an obstacle, but instead reproduces the intrinsic temperature of a body or the heat flow caused by a heat source [2]. All the bodies with a temperature different from absolute zero emit a specific energy caused by the movement of the molecules. The intensity of this movement changes with the change of temperature of the body: the molecules move faster with high temperatures. This movement is also synonymous of a movement of electrical charges that generates electromagnetic radiation in the wavelengths of the infrared band (from 0.8 to 15 μm). The infrared camera captures thus this energy and converts it into an electronic signal, which is processed by a software and transformed into a thermal image (**Erreur ! Source du renvoi introuvable.**). The image is used for temperature calculations and to evaluate the severity of the thermal problem, thanks to the possibility of quantifying the captured heat very precisely.

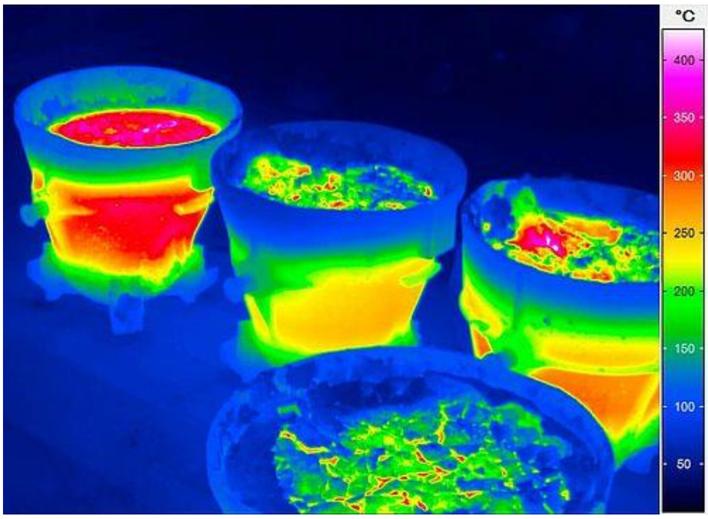

Figure 3: Example of an infrared image of four full steel ladles.

For this type of experiment, a very important parameter is the emissivity ε of the analysed object, which is the ability of the body to emit infrared radiation, see Equ. 1. It is defined as the ratio between the power flow ε_{λ} emitted at a wavelength λ by a real body at a given temperature T and the power flow $\varepsilon_{\lambda b}$ that would be emitted at the same wavelength λ by a black body brought to same temperature T. A black body is able to absorb any incident radiation regardless of its wavelength and to emit radiations at all wavelengths [3].

$$\varepsilon = \frac{\varepsilon_{\lambda}}{\varepsilon_{\lambda b}} \qquad \textit{Equ. 1}$$

The ε values of many of the most common materials can be easily found in the literature (Table 3 and Table 4).

Table 3: Emissivity of different materials – Part 1 of 2 – Metals – Source: Omegascope Company [5]

Material	Temp °F (°C)	ε Emissivity
Alloys		
20-Ni, 24-CR, 55-FE, Oxid.	392 (200)	.90
20-Ni, 24-CR, 55-FE, Oxid.	932 (500)	.97
60-Ni , 12-CR, 28-FE, Oxid.	518 (270)	.89
60-Ni , 12-CR, 28-FE, Oxid.	1040 (560)	.82
80-Ni, 20-CR, Oxidized	212 (100)	.87
80-Ni, 20-CR, Oxidized	1112 (600)	.87
80-Ni, 20-CR, Oxidized	2372 (1300)	.89
Aluminum		
Unoxidized	77 (25)	.02
Unoxidized	212 (100)	.03
Unoxidized	932 (500)	.06
Oxidized	390 (199)	.11
Oxidized	1110 (599)	.19
Oxidized at 599°C (1110°F)	390 (199)	.11
Oxidized at 599°C (1110°F)	1110 (599)	.19
Heavily Oxidized	200 (93)	.20
Heavily Oxidized	940 (504)	.31
Highly Polished	212 (100)	.09
Roughly Polished	212 (100)	.18
Commercial Sheet	212 (100)	.09
Highly Polished Plate	440 (227)	.04
Highly Polished Plate	1070 (577)	.06
Bright Rolled Plate	338 (170)	.04
Bright Rolled Plate	932 (500)	.05
Alloy A3003, Oxidized	600 (316)	.40
Alloy A3003, Oxidized	900 (482)	.40
Alloy 1100-0	200-800 (93-427)	.05
Alloy 24ST	75 (24)	.09
Alloy 24ST, Polished	75 (24)	.09
Alloy 75ST	75 (24)	.11
Alloy 75ST, Polished	75 (24)	.08
Bismuth, Bright	176 (80)	.34
Bismuth, Unoxidized	77 (25)	.05
Bismuth, Unoxidized	212 (100)	.06
Brass		
73% Cu, 27% Zn, Polished	476 (247)	.03
73% Cu, 27% Zn, Polished	674 (357)	.03
62% Cu, 37% Zn, Polished	494 (257)	.03
62% Cu, 37% Zn, Polished	710 (377)	.04
83% Cu, 17% Zn, Polished	530 (277)	.03
Matte	68 (20)	.07
Burnished to Brown Color	68 (20)	.40
Cu-Zn, Brass Oxidized	392 (200)	.61
Cu-Zn, Brass Oxidized	752 (400)	.60
Cu-Zn, Brass Oxidized	1112 (600)	.61
Unoxidized	77 (25)	.04
Unoxidized	212 (100)	.04
Cadmium	77 (25)	.02
Carbon		
Lampblack	77 (25)	.95
Unoxidized	77 (25)	.81
Unoxidized	212 (100)	.81
Unoxidized	932 (500)	.79
Candle Soot	250 (121)	.95
Filament	500 (260)	.95
Graphitized	212 (100)	.76
Graphitized	572 (300)	.75
Graphitized	932 (500)	.71
Chromium	100 (38)	.08
Chromium	1000 (538)	.26
Chromium, Polished	302 (150)	.06
Cobalt, Unoxidized	932 (500)	.13
Cobalt, Unoxidized	1832 (1000)	.23
Columbium, Unoxidized	1500 (816)	.19
Columbium, Unoxidized	2000 (1093)	.24
Copper		
Cuprous Oxide	100 (38)	.87
Cuprous Oxide	500 (260)	.83
Cuprous Oxide	1000 (538)	.77
Black, Oxidized	100 (38)	.78
Etched	100 (38)	.09
Matte	100 (38)	.22
Roughly Polished	100 (38)	.07

Material	Temp °F (°C)	ε Emissivity
Polished	100 (38)	.03
Highly Polished	100 (38)	.02
Rolled	100 (38)	.64
Rough	100 (38)	.74
Molten	1000 (538)	.15
Molten	1970 (1077)	.16
Molten	2230 (1221)	.13
Nickel Plated	100-500 (38-260)	.37
Dow Metal	0.4-600 (–18-316)	.15
Gold		
Enamel	212 (100)	.37
Plate (.0001)		
Plate on .0005 Silver	200-750 (93-399)	.11-.14
Plate on .0005 Nickel	200-750 (93-399)	.07-.09
Polished	100-500 (38-260)	.02
Polished	1000-2000 (538-1093)	.03
Haynes Alloy C,		
Oxidized	600-2000 (316-1093)	.90-.96
Haynes Alloy 25,		
Oxidized	600-2000 (316-1093)	.86-.89
Haynes Alloy X,		
Oxidized	600-2000 (316-1093)	.85-.88
Inconel Sheet	1000 (538)	.28
Inconel Sheet	1200 (649)	.42
Inconel Sheet	1400 (760)	.58
Inconel X, Polished	75 (24)	.19
Inconel B, Polished	75 (24)	.21
Iron		
Oxidized	212 (100)	.74
Oxidized	930 (499)	.84
Oxidized	2190 (1199)	.89
Unoxidized	212 (100)	.05
Red Rust	77 (25)	.70
Rusted	77 (25)	.65
Liquid	2760-3220 (1516-1771)	.42-.45
Cast Iron		
Oxidized	390 (199)	.64
Oxidized	1110 (599)	.78
Unoxidized	212 (100)	.21
Strong Oxidation	40 (104)	.95
Strong Oxidation	482 (250)	.95
Liquid	2795 (1535)	.29
Wrought Iron		
Dull	77 (25)	.94
Dull	660 (349)	.94
Smooth	100 (38)	.35
Polished	100 (38)	.28
Lead		
Polished	100-500 (38-260)	.06-.08
Rough	100 (38)	.43
Oxidized	100 (38)	.43
Oxidized at 1100°F	100 (38)	.63
Gray Oxidized	100 (38)	.28
Magnesium	100-500 (38-260)	.07-.13
Magnesium Oxide	1880-3140 (1027-1727)	.16-.20
Mercury	32 (0)	.09
Mercury	77 (25)	.10
Mercury	100 (38)	.10
	212 (100)	.12
Molybdenum	100 (38)	.06
Molybdenum	500 (260)	.08
Molybdenum	1000 (538)	.11
Molybdenum	2000 (1093)	.18
" Oxidized at 1000°F	600 (316)	.80
" Oxidized at 1000°F	700 (371)	.84
" Oxidized at 1000°F	800 (427)	.84
" Oxidized at 1000°F	900 (482)	.83
" Oxidized at 1000°F	1000 (538)	.82
Monel, Ni-Cu	392 (200)	.41
Monel, Ni-Cu	752 (400)	.44
Monel, Ni-Cu	1112 (600)	.46
Monel, Ni-Cu Oxidized	68 (20)	.43

Material	Temp °F (°C)	ε Emissivity
Monel, Ni-Cu Oxid. at 1110°F	1110 (599)	.46
Nickel		
Polished	100 (38)	.05
Oxidized	100-500 (38-260)	.31-.46
Unoxidized	77 (25)	.05
Unoxidized	212 (100)	.06
Unoxidized	932 (500)	.12
Unoxidized	1832 (1000)	.19
Electrolytic	100 (38)	.04
Electrolytic	500 (260)	.06
Electrolytic	1000 (538)	.10
Electrolytic	2000 (1093)	.16
Nickel Oxide	1000-2000 (538-1093)	.59-.86
Palladium Plate (.00005 on .0005 silver)	200-750 (93-399)	.16-.17
Platinum	100 (38)	.05
Platinum	500 (260)	.05
Platinum	1000 (538)	.10
Platinum, Black	100 (38)	.93
Platinum, Black	500 (260)	.96
Platinum, Black	2000 (1093)	.97
" Oxidized at 1100°F	500 (260)	.07
"	1000 (538)	.11
Rhodium Flash (0.0002 on 0.0005 Ni)	200-700 (93-371)	.10-.18
Silver		
Plate (0.0005 on Ni)	200-700 (93-371)	.06-.07
Polished	100 (38)	.01
Polished	500 (260)	.02
Polished	1000 (538)	.03
Polished	2000 (1093)	.03
Steel		
Cold Rolled	200 (93)	.75-.85
Ground Sheet	1720-2010 (938-1099)	.55-.61
Polished Sheet	100 (38)	.07
Polished Sheet	500 (260)	.10
Polished Sheet	1000 (538)	.14
Mild Steel, Polished	75 (24)	.10
Mild Steel, Smooth	75 (24)	.12
Mild Steel, Liquid	2910-3270 (1599-1793)	.28
Steel, Unoxidized	212 (100)	.08
Steel, Oxidized	77 (25)	.80
Steel Alloys		
Type 301, Polished	75 (24)	.27
Type 301, Polished	450 (232)	.57
Type 301, Polished	1740 (949)	.55
Type 303, Oxidized	600-2000 (316-1093)	.74-.87
Type 310, Rolled	1500-2100 (816-1149)	.56-.81
Type 316, Polished	75 (24)	.28
Type 316, Polished	450 (232)	.57
Type 316, Polished	1740 (949)	.66
Type 321	200-800 (93-427)	.27-.32
Type 321 Polished	300-1500 (149-815)	.18-.49
Type 321 w/BK Oxide	200-800 (93-427)	.66-.76
Type 347, Oxidized	600-2000 (316-1093)	.87-.91
Type 350	200-800 (93-427)	.18-.27
Type 350 Polished	300-1800 (149-982)	.11-.35
Type 446, Polished	300-1500 (149-815)	.15-.37
Type 17-7 PH	200-600 (93-316)	.44-.51
Type 17-7 PH		
Polished	300-1500 (149-815)	.09-.16
Type C1020, Oxidized	600-2000 (316-1093)	.87-.91
Type PH-15-7 MO	300-1200 (149-649)	.07-.19
Stellite, Polished	68 (20)	.18
Tantalum, Unoxidized	1340 (727)	.14
"	2000 (1093)	.19
"	3600 (1982)	.26
"	5306 (2930)	.30
Tin, Unoxidized	77 (25)	.04
"	212 (100)	.05
Tinned Iron, Bright	76 (24)	.05
	212 (100)	.08

Table 4: Emissivity of different materials – Part 2 of 2 – Non-metals – Source: Omegascope Company [5]

Material	Temp °F (°C)	ε Emmissivity	Material	Temp °F (°C)	ε Emmissivity	Material	Temp °F (°C)	ε Emmissivity
Adobe	68 (20)	.90	Granite	70 (21)	.45	Paints, Oil		
Asbestos			Gravel	100 (38)	.28	All colors	200 (93)	.92-.96
Board	100 (38)	.96	Ice, Smooth	32 (0)	.97	Black	200 (93)	.92
Cement	32-392 (0-200)	.96	Ice, Rough	32 (0)	.98	Black Gloss	70 (21)	.90
Cement, Red	2500 (1371)	.67	Lacquer			Camouflage Green	125 (52)	.85
Cement, White	2500 (1371)	.65	Black	200 (93)	.96	Flat Black	80 (27)	.88
Cloth	199 (93)	.90	Blue, on Al Foil	100 (38)	.78	Flat White	80 (27)	.91
Paper	100-700 (38-371)	.93	Clear, on Al Foil (2 coats)	200 (93)	.08 (.09)	Gray-Green	70 (21)	.95
Slate	68 (20)	.97	Clear, on Bright Cu	200 (93)	.66	Green	200 (93)	.95
Asphalt, pavement	100 (38)	.93	Clear, on Tarnished Cu	200 (93)	.64	Lamp Black	209 (98)	.96
Asphalt, tar paper	68 (20)	.93	Red, on Al Foil (2 coats)	100 (38)	.61 (.74)	Red	200 (93)	.95
Basalt	68 (20)	.72	White	200 (93)	.95	White	200 (93)	.94
Brick			White, on Al Foil (2 coats)	100 (38)	.69 (.88)	Quartz, Rough, Fused	70 (21)	.93
Red, rough	70 (21)	.93	Yellow, on Al Foil (2 coats)	100 (38)	.57 (.79)	Glass, 1.98 mm	540 (282)	.90
Gault Cream	2500-5000 (1371-2760)	.26-.30	Lime Mortar	100-500 (38-260)	.90-.92	Glass, 1.98 mm	1540 (838)	.41
Fire Clay	2500 (1371)	.75	Limestone	100 (38)	.95	Glass, 6.88 mm	540 (282)	.93
Light Buff	1000 (538)	.80	Marble, White	100 (38)	.95	Glass, 6.88 mm	1540 (838)	.47
Lime Clay	2500 (1371)	.43	" Smooth, White	100 (38)	.56	Opaque	570 (299)	.92
Fire Brick	1832 (1000)	.75-.80	" Polished Gray	100 (38)	.75	Opaque	1540 (838)	.68
Magnesite, Refractory	1832 (1000)	.38	Mica	100 (38)	.75	Red Lead	212 (100)	.93
Gray Brick	2012 (1100)	.75	Oil on Nickel			Rubber, Hard	74 (23)	.94
Silica, Glazed	2000 (1093)	.88	0.001 Film	72 (22)	.27	Rubber, Soft, Gray	76 (24)	.86
Silica, Unglazed	2000 (1093)	.80	0.002 "	72 (22)	.46	Sand	68 (20)	.76
Sandlime	2500-5000 (1371-2760)	.59-.63	0.005 "	72 (22)	.72	Sandstone	100 (38)	.67
Carborundum	1850 (1010)	.92	Thick "	72 (22)	.82	Sandstone, Red	100 (38)	.60-.83
Ceramic			Oil, Linseed			Sawdust	68 (20)	.75
Alumina on Inconel	800-2000 (427-1093)	.69-.45	On Al Foil, uncoated	250 (121)	.09	Shale	68 (20)	.69
Earthenware, Glazed	70 (21)	.90	On Al Foil, 1 coat	250 (121)	.56	Silica,Glazed	1832 (1000)	.85
Earthenware, Matte	70 (21)	.93	On Al Foil, 2 coats	250 (121)	.51	Silica, Unglazed	2012 (1100)	.75
Greens No. 5210-2C	200-750 (93-399)	.89-.82	On Polished Iron, .001 Film	100 (38)	.22	Silicon Carbide	300-1200 (149-649)	.83-.96
Coating No. C20A	200-750 (93-399)	.73-.67	On Polished Iron, .002 Film	100 (38)	.45	Silk Cloth	68 (20)	.78
Porcelain	72 (22)	.92	On Polished Iron, .004 Film	100 (38)	.65	Slate	100 (38)	.67-.80
White Al2O3	200 (93)	.90	On Polished Iron, Thick Film	100 (38)	.83	Snow, Fine Particles	20 (–7)	.82
Zirconia on Inconel	800-2000 (427-1093)	.62-.45	Paints			Snow, Granular	18 (–8)	.89
Clay	68 (20)	.39	Blue, Cu2O3	75 (24)	.94	Soil		
" Fired	158 (70)	.91	Black, CuO	75 (24)	.96	Surface	100 (38)	.38
" Shale	68 (20)	.69	Green, Cu2O3	75 (24)	.92	Black Loam	68 (20)	.66
" Tiles, Light Red	2500-5000 (1371-2760)	.32-.34	Red, Fe2O3	75 (24)	.91	Plowed Field	68 (20)	.38
" Tiles, Red	2500-5000 (1371-2760)	.40-.51	White, Al2O3	75 (24)	.94	Soot		
" Tiles, Dark Purple	2500-5000 (1371-2760)	.78	White, Y2O3	75 (24)	.90	Acetylene	75 (24)	.97
Concrete			White, ZnO	75 (24)	.95	Camphor	75 (24)	.94
Rough	32-2000 (0-1093)	.94	White, MgCO3	75 (24)	.91	Candle	250 (121)	.95
Tiles, Natural	2500-5000 (1371-2760)	.63-.62	White, ZrO2	75 (24)	.95	Coal	68 (20)	.95
" Brown	2500-5000 (1371-2760)	.87-.83	White, ThO2	75 (24)	.90	Stonework	100 (38)	.93
" Black	2500-5000 (1371-2760)	.94-.91	White, MgO	75 (24)	.91	Water	100 (38)	.67
Cotton Cloth	68 (20)	.77	White, PbCO3	75 (24)	.93	Waterglass	68 (20)	.96
Dolomite Lime	68 (20)	.41	Yellow, PbO	75 (24)	.90	Wood	Low	.80-.90
Emery Corundum	176 (80)	.86	Yellow, PbCrO4	75 (24)	.93	Beech Planed	158 (70)	.94
Glass			Paints, Aluminium	100 (38)	.27-.67	Oak, Planed	100 (38)	.91
Convex D	212 (100)	.80	10% Al	100 (38)	.52	Spruce, Sanded	100 (38)	.89
Convex D	600 (316)	.80	26% Al	100 (38)	.30			
Convex D	932 (500)	.76	Dow XP-310	200 (93)	.22			
Nonex	212 (100)	.82	Paints, Bronze	Low	.34-.80			
Nonex	600 (316)	.82	Gum Varnish (2 coats)	70 (21)	.53			
Nonex	932 (500)	.78	Gum Varnish (3 coats)	70 (21)	.50			
Smooth	32-200 (0-93)	.92-.94	Cellulose Binder (2 coats)	70 (21)	.34			

However, these values are not always useful when dealing with an IR system for two main reasons:

- The table does not contain any information about the direction and the wavelength that the emissivity refers to.
- State of the viewed surface: tables presented in literature include terms like polished, cast, rolled, oxidized, heavily oxidized etc., and emissivity values range inside very large intervals; such values cannot thus be used to get accurate temperature measurements.

A better way is to directly measure the emissivity with the same IR camera. The procedure involves simply in comparing the radiation emitted by the sample material and that emitted by a blackbody at the same temperature. Almost every IR thermographic system is equipped with software for emissivity calculations.

When considering the calibration of numerical models, the infrared cameras present some advantages compared to the use of thermocouples. This equipment, in fact, provides full field measurement of the temperatures, while thermocouples provide punctual measurements. If the problem involves a significant gradient of temperatures (an example is described in the Paragraph 3.1.1), a large number of thermocouples would be necessary to evaluate the system, whereas only one IR camera would be required to provide all the necessary measurements. A drawback is the limitation of measuring temperatures inside the linings and between the layers, so in such cases, thermocouples are more suitable.

A second parameter to consider when using the IR camera is the environment or more specifically the specific transmissivity of the path made by the radiation. The atmosphere, for example, has three transmission windows in the infrared (near, medium, far) and it is in these wavelength bands that the detectors are optimized. It must also be considered that certain components of the atmosphere, such as water vapour and carbon dioxide, absorb infrared radiation at a certain wavelength and cause transmission losses.

2.3. Laser scanner

The laser scanner technique does not allow the direct measurement of temperature, this is evaluated using a pyrometric channel. This channel measures the heat radiation of the material at different hot spots. The laser scanner equipment was invented to measure the distance between the laser source and the “target” by sending an infrared laser pulse from outside the ladle to the wall and the bottom (Figure 4) [4]. Knowing the original dimensions, the shape and any deformations of the ladle, it is then possible to evaluate the reduction of the thickness. This control is really important in order to avoid breakouts which can have serious consequences in terms of production (economical aspect) and general safety of personnel (human aspect). In fact, the refractory bricks are continuously subjected to corrosive attacks by hot liquid steel and slag that cause a reduction in thickness of the lining.

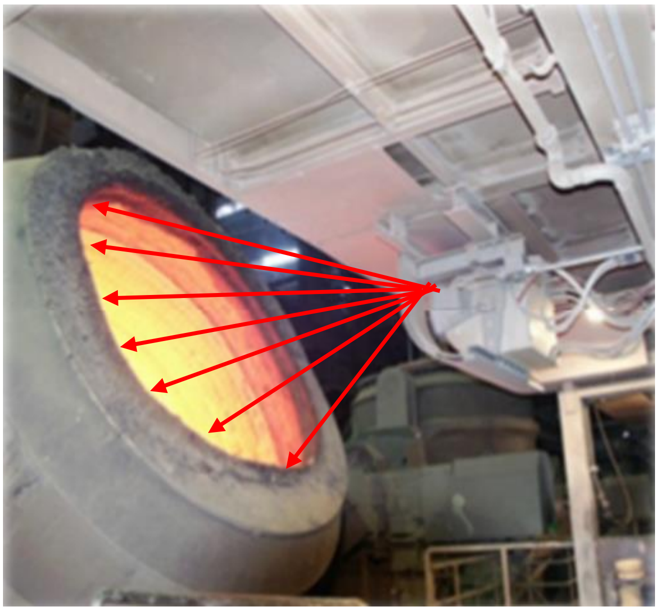

Figure 4: Laser scanner measures on the internal surface of the ladle from the outside the steel ladle.

Two problems can be detected:

- the accuracy of the measurements depends on the angle of incidence of the laser beam;
- the shadowed area under the mouth is not accessible for the laser beam.

The second disadvantage has an impact on the measurability of the slag zone, a very important area in ladle lining relating to the risk of a breakthrough. To overcome the above problem, a laser head system has been developed [4].

The entire measurement takes less than 3 minutes and it can be divided in three steps (Figure 5):

a) the laser head is positioned such that the laser scanner sees the outer contour and a part of the mouth of the ladle in order to find the exact position of the ladle by using a “3D – structure finding” software;
b) the second scan is carried out in front of the mouth to measure the area of the bottom of the ladle;
c) the laser head moves completely through the mouth inside the hot ladle and it measures the ladle wall lining with a 360° rotating laser scanner; each scan takes only 20 seconds.

Once the measurement is finished, the head returns at the position zero. The data are collected (generally 3.9 million points with accuracy better than 5 mm) and processed.

a)

b)

c)

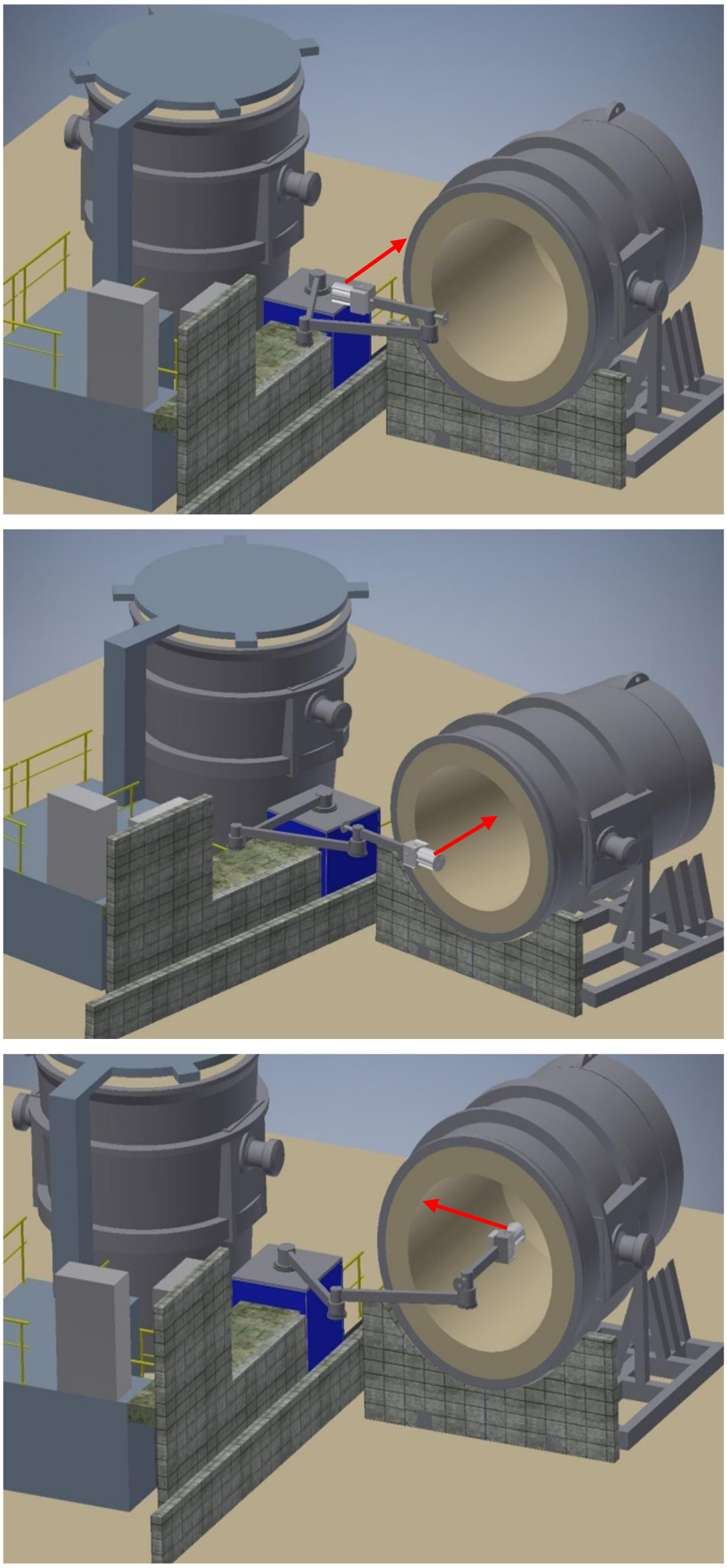

Figure 5: Measurement procedure.

European Commission
Horizon 2020
European Union funding
for Research & Innovation

3. Application in ATHOR project

The devices presented is this document are being used to perform the thermal instrumentation of laboratory tests and in-situ measurements in industrial scale. Some cases are detailed in the next sections.

3.1. Laboratory experiments

3.1.1. ATHORNA Device

The ATHORNA Device (Advanced measurements for in-situ THermo-mechanical monitoring of large sample uNder thermal gradient) is being developing inside the scope of ATHOR Project. The objective of the equipment is to study the thermo-mechanical behaviour of refractory materials under thermal gradient and consequently evaluate their resistance to thermal shocks.

A cylindrical sample with a diameter of ø100 mm and thickness of 10mm to 20mm is subjected to CO_2 laser pulses. The power discharged by the laser can vary from 50W up to 2000W, which leads to an increase in sample temperature, the exposed face may reach temperatures as high as the temperatures in service conditions of refractory materials. The strain fields at the bottom face are evaluated using a stereoscopic optical system with two cameras. The temperatures at the bottom face are measured using one infrared camera. Acoustic emission sensors will be installed in the future to evaluate the acoustic activity of the sample and to track the cracks. The experimental setup of the ATHORNA device is presented in Figure 6.

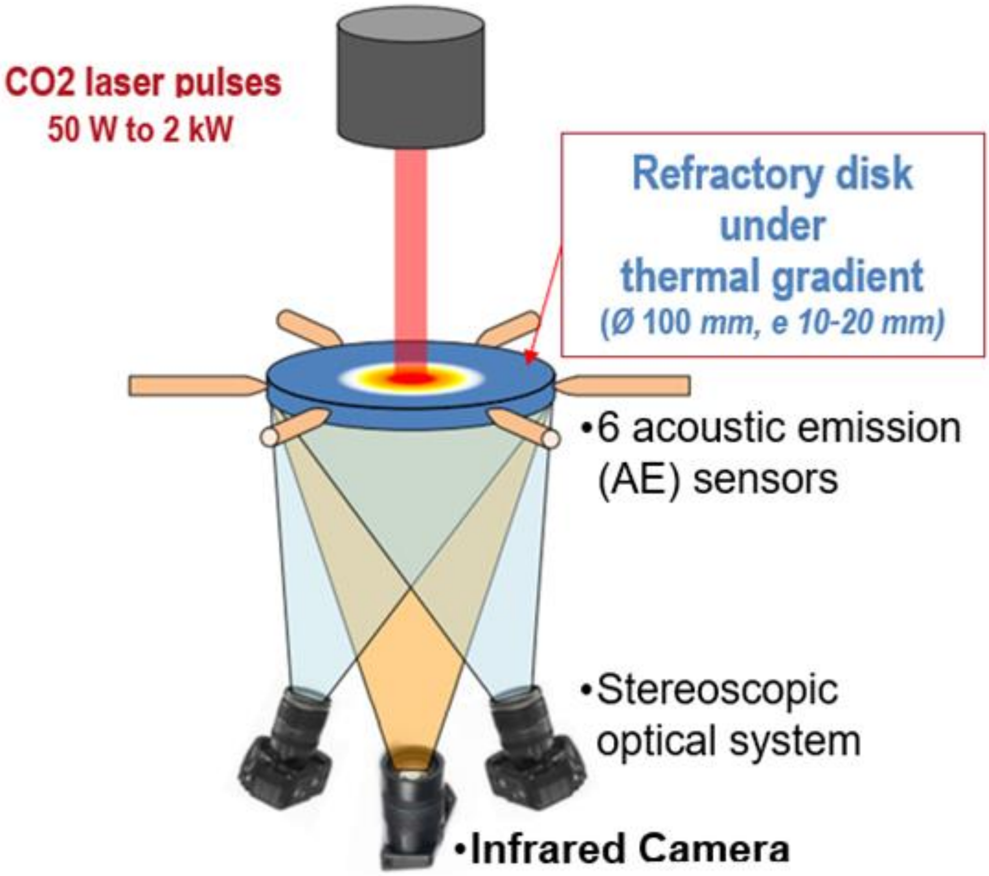

Figure 6: Experimental setup – ATHORNA Device

The laser pulses increase the temperature at the centre of the sample, which leads to two different temperature gradients:

i) **Diametral temperature gradient:** the higher temperatures at the centre of the sample result in a restrained thermal expansion. This leads to compression stresses at the centre of the sample and tangential tensile stresses at the borders of the sample. The tangential tensile stresses lead to crack initiation and propagation.

ii) **Temperature gradient across the thickness of the sample:** the higher temperatures at the top face (exposed-face) leads to a thermal bowing of the sample.

European Commission | Horizon 2020 European Union funding for Research & Innovation

The measurement of temperatures by the IR camera at the bottom face is presented in Figure 7. Figure 7 (a) and (c) represent the thermal image and the diametral temperature at the beginning of the test, respectively. Figure 7 (b) and (d) present the measurements during laser application.

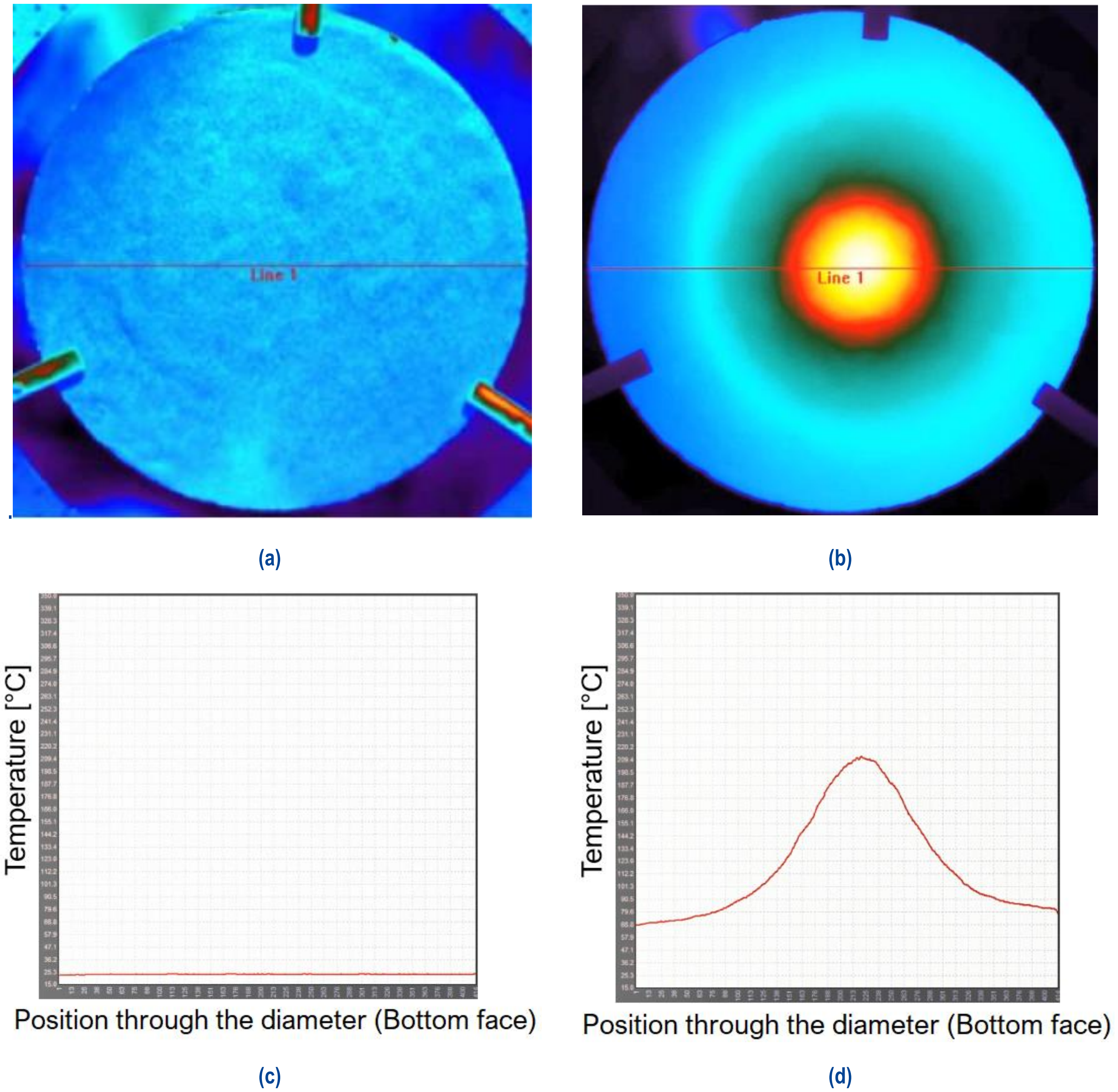

Figure 7: Temperature measurements using IR Cameras on ATHORNA device: (a) IR Camera image – Beginning of the test; (b) IR Camera image – During laser application; (c) Diametral temperature – Beginning of the test; (d) Diametral temperature – During laser application

The Digital Image Correlations (DIC) technique allows the measurement of the total strain in the sample (ε_{total}). However, in order to best analyse the problem it is necessary to decouple the strains components in mechanical strains (ε_{mec}) and thermal strains ($\varepsilon_{thermal}$), as described in Equ. 2:

$$\varepsilon_{total} = \varepsilon_{mec} + \varepsilon_{thermal} \qquad \textit{Equ. 2}$$

The thermal strains can be predicted based on the temperature fields and the thermal expansion coefficient of the material. Therefore, the thermal instrumentation is important for the accuracy of the study. The procedure used to determine the mechanical strain fields is presented at Figure 8.

European Commission
Horizon 2020
European Union funding
for Research & Innovation

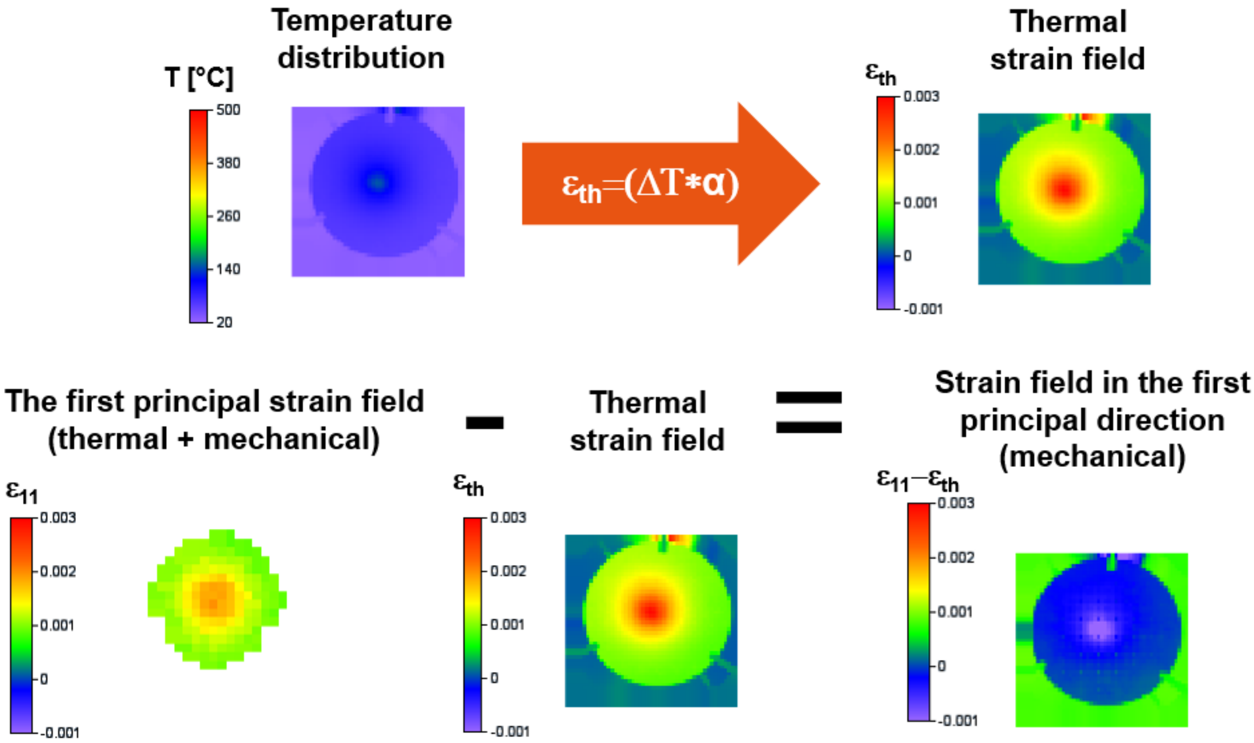

Figure 8: Decoupling thermal strain from total strain

Moreover, numerical models are being used to predict the behaviour of the material in the regions where the instrumentation (thermal and mechanical) is not applicable, such as in the hot face and inside the sample. The calibration of the numerical models are important to increase the agreement between the experimental and numerical results. The IR camera is used to validate the numerical heat transfer analysis.

Figure 9 (a) presents the temperature at the centre of the bottom face, the experimental measured and numerical predicted values are presented in blue and green, respectively. Figure 9 (b) presents the diametral temperature at the beginning and by the end of cycle C15. The measured temperatures at the bottom face are presented by the dashed blue line, the predicted temperatures at the bottom and top face are presented by the continuous line in blue and red, respectively.

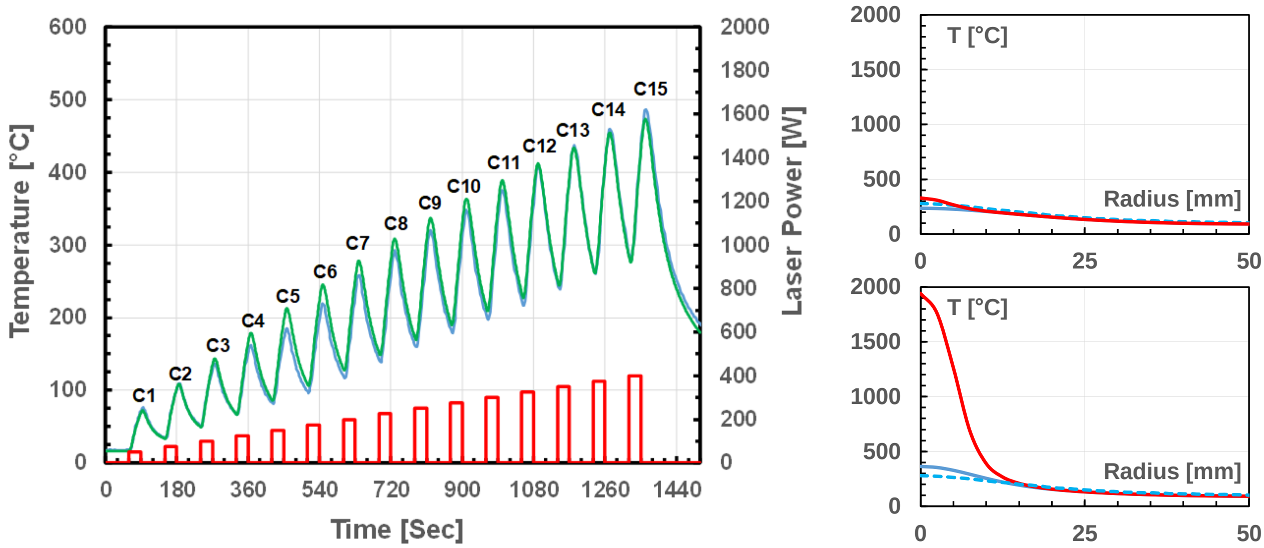

(a) (b)

Figure 9: Temperatures measurements – Experimental and Numerical values: (a) Temperature at the centre of the sample versus time; (b) diametral temperature at cycle C15.

European Commission | Horizon 2020 European Union funding for Research & Innovation

3.1.2. Compressive test in masonry wallets

Two sets of compressive tests in masonry wallets are foreseen inside the scope of ATHOR Project:

i) **Uniaxial compressive tests:** The compressive load will be applied in one direction. These tests will take place at the ISISE laboratory of the University of Coimbra, in Coimbra – Portugal.

ii) **Biaxial compressive tests:** The compressive load will be applied in two orthogonal directions. These tests will take place the Research Centre of RHI-Magnesita, in Leoben – Austria.

The experimental setup of these tests are presented in Figure 10 and Figure 11. The thermal instrumentation to be used in the experimental layout is presented.

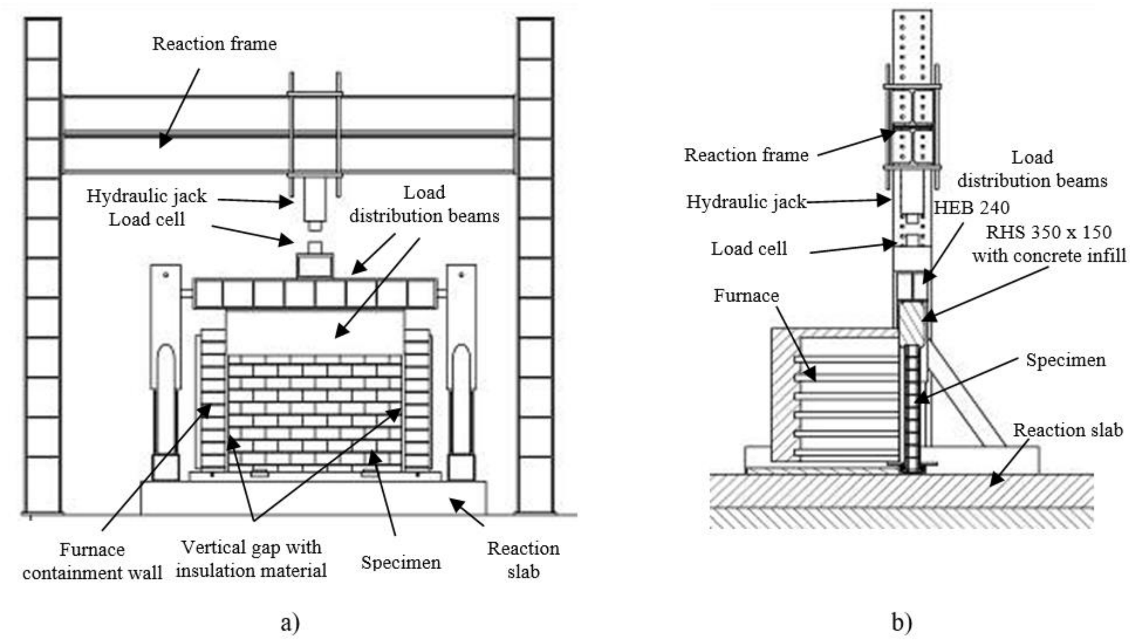

Figure 10: Experimental setup: Uniaxial compressive test: (a) Front view (b) Cut (2017) [6]

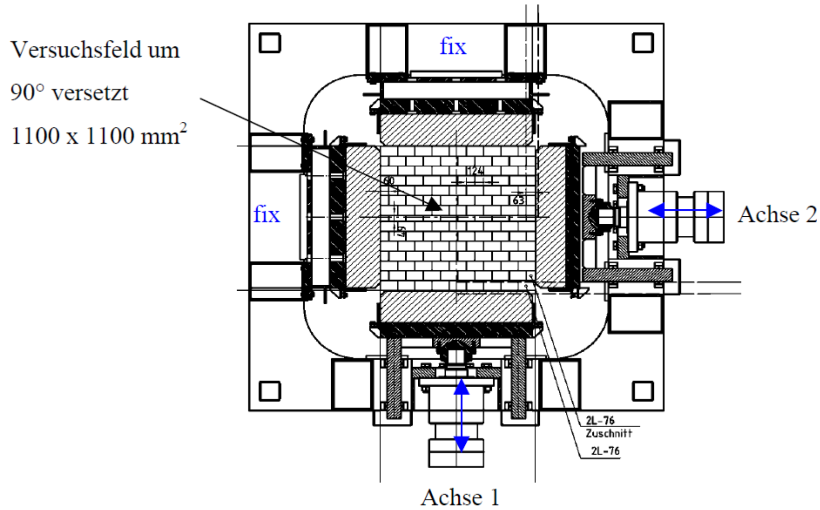

Figure 11: Experimental setup: Biaxial compressive test (2006) [7]

3.1.2.1. *Thermal instrumentation of the uniaxial compressive test*

The uniaxial compressive tests will last for four hours and the temperature of the furnace is limited to 1200 ºC. An electrical furnace will be used to heat the one face of the wall(hot face), the other face (cold face) will be used for the thermal instrumentation. In order to design the experimental layout and to determine the thermal instrumentation, some predictive models were used. The predicted temperatures at the hot face (HF) and at the cold face (CF) are presented in Figure 12 (a). Figure 12 (b) presents the distribution of temperatures at by the end of the test.

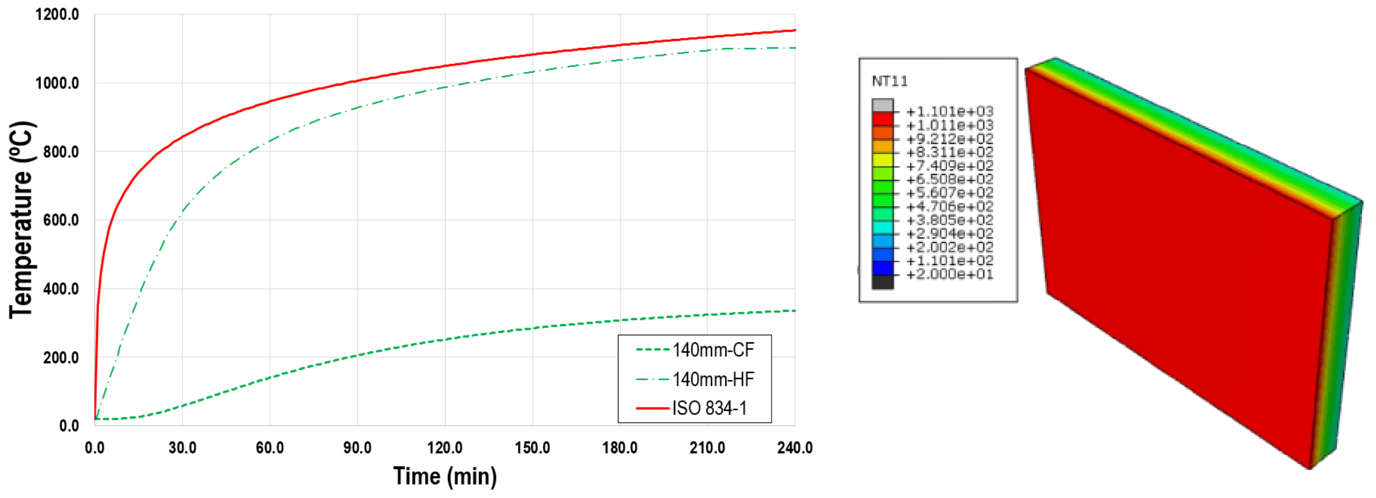

(a) **(b)**

Figure 12: Uniaxial compressive test: Prediction of temperatures: (a) Temperature vs time, (b) Temperature distribution.

Based on the temperatures fields by the end of the test, the thermal instrumentation was defined. Type K thermocouples will be used. This type of thermocouples (Nickel-Chromium / Nickel-Alumel) can operate in temperatures up to 1260ºC and present good accuracy (+/- 2.2C or +/- 0.75%). Moreover, this equipment is relatively cheap and easy to weld and install. The thermocouples will be installed in different positions of the wall and in both faces (hot face and cold face), in order to evaluate the temperatures and thermal gradients across the thickness of the wall, as presented in Figure 13.

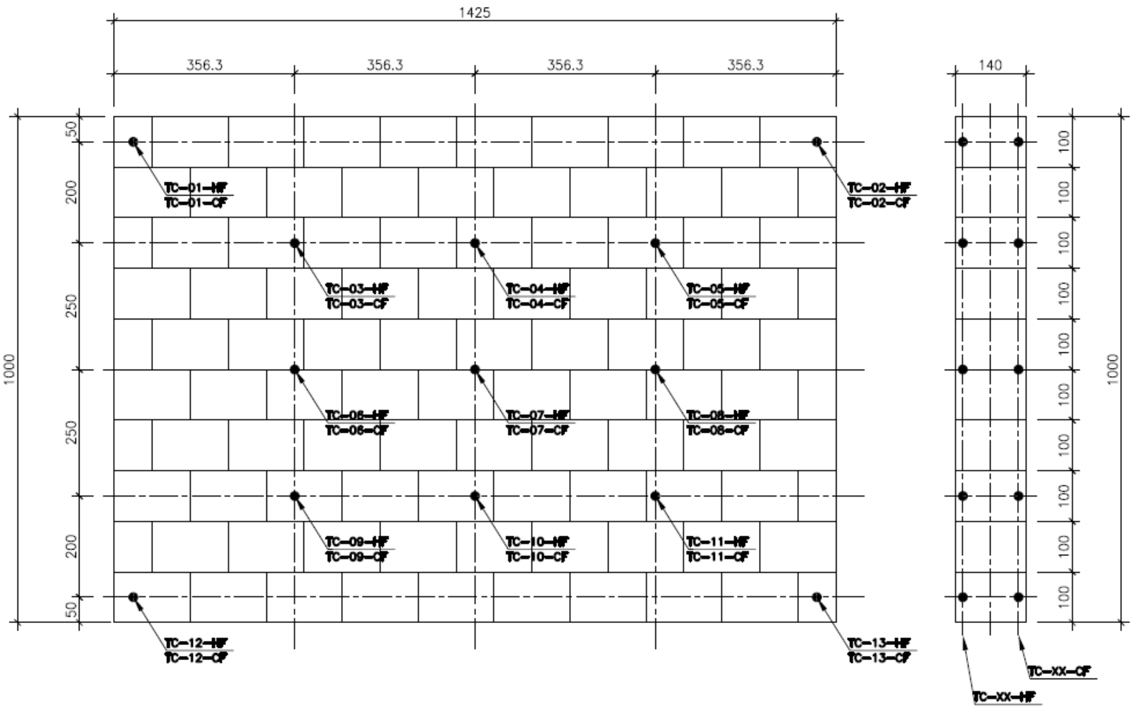

Figure 13: Uniaxial compressive test: Thermal instrumentation

3.1.2.2. Thermal instrumentation of the biaxial compressive test

The biaxial compressive tests aims to represent the service conditions of masonry linings. The heating rate of 25ºC/h will be used, representing the heating rate usually used in industrial linings. The samples will be tested in different temperatures: *i*) Room temperature, *ii*) 600ºC, *iii*) 1.000 ºC and *iv*) 1.500 ºC.

The thermal instrumentation was defined based on the temperatures of the test. Type K thermocouples will be used for the tests at 600ºC and 1000ºC. However, the tests at 1500 ºC exceed the working temperature of these thermocouples (1260 ºC): Therefore it will be necessary the use of another type of thermocouple, as presented in Table 1.

The thermocouples will be installed in different positions of the wall and in both faces (hot face and cold face), in order to evaluate the temperatures and thermal gradients across the thickness of the wall (Figure 14).

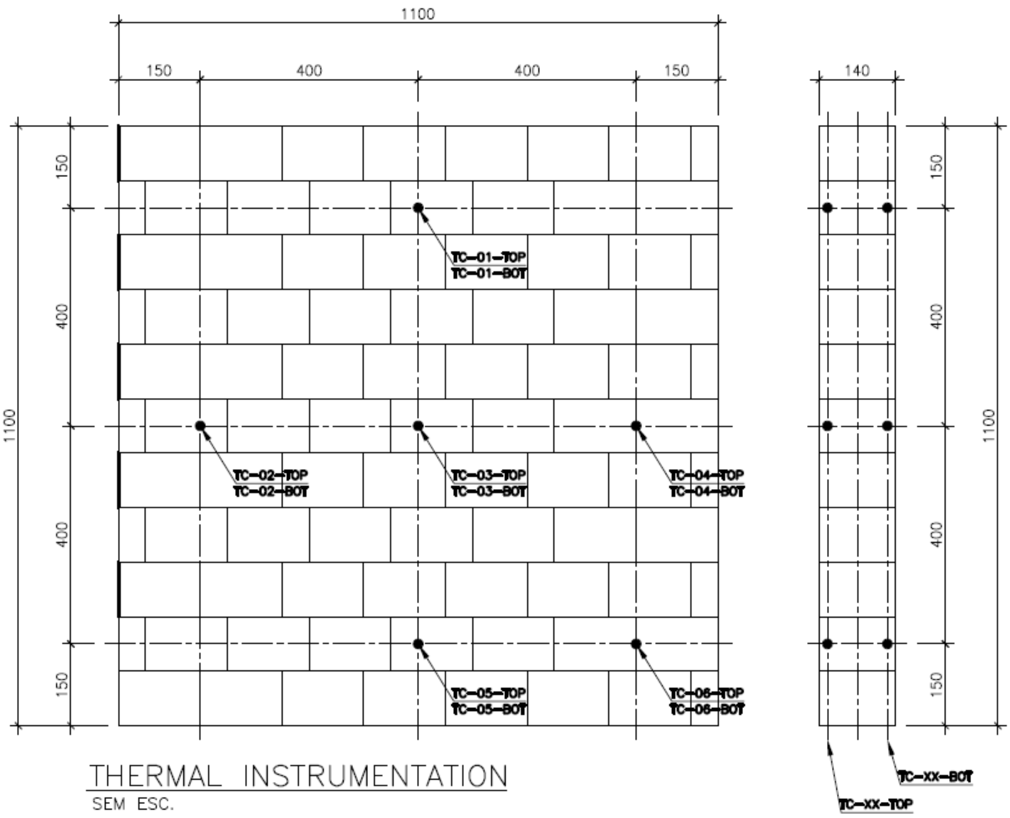

Figure 14: Biaxial compressive test: Thermal instrumentation

3.2. In-situ measurements

A 3D pilot scale model will be constructed inside the scope of ATHOR Project. It consists of a cylindrical steel shell with a welded plane bottom. The refractory lining will be arranged in concentric layers at the side of the steel ladle and stacked layers at the bottom. The schematic drawing of the pilot ladle is presented in Figure 15.

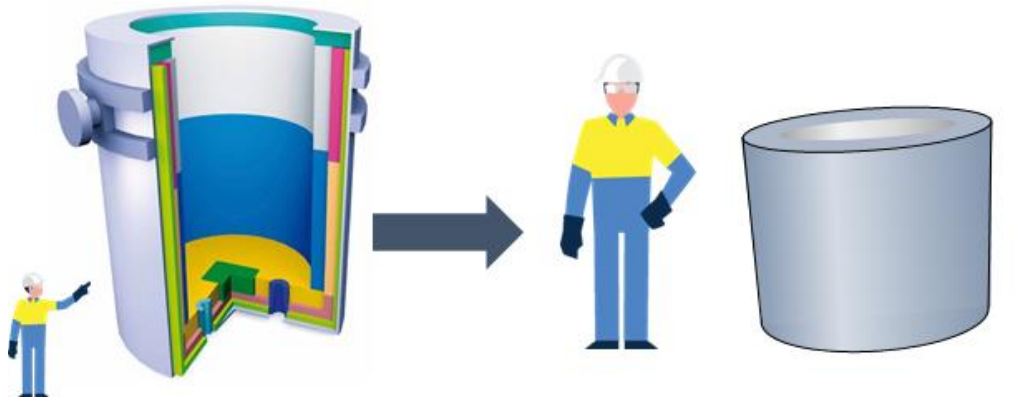

Figure 15: Pilot Steel Ladle.

To perform the numerical calibration and the validation of the developed models, it will be necessary to measure the temperature distribution and the temperature fluxes. Some predictive models are being used to design the pilot ladle and to determine the thermal instrumentation of the system, as presented in Figure 16.

European Commission
Horizon 2020
European Union funding
for Research & Innovation

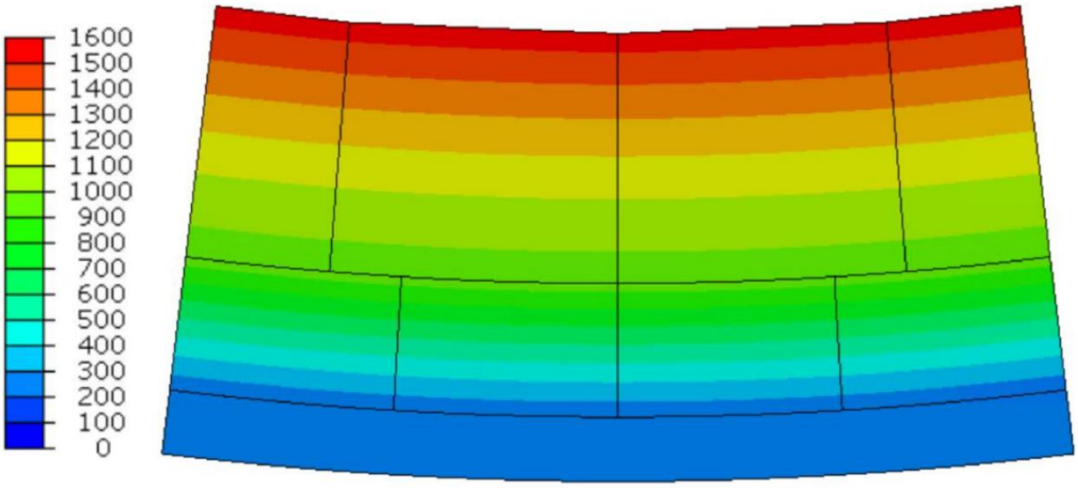

Figure 16: Prediction of temperatures (ºC)

Based on the predicted temperatures, the thermal instrumentation comprises:

- Type K thermocouples: the thermocouples will be installed in the steel shell and between the refractory layers aiming to measure the temperature gradient across the thickness of the ladle.
- IR Cameras: these devices will be used to measure the temperature fields at the wear layer and also at the steel shell.

More information about the pilot steel ladle is presented in Deliverable D1.5 and D1.6.

4. Conclusions

This document summarizes the current methodology used for thermal instrumentation on industrial vessels, including suitable acquisition equipment and techniques. This deliverable is the output of the "Task 1.1 – Thermal Instrumentation" as a task of "WP1 - Improvements of measurements tools".

Section 2 described the techniques used for thermal instrumentation currently used in industrial measurements and in academic researches. Some techniques, such as thermocouples, infrared cameras and laser scanning, were presented. Section 3 described how these techniques are being used inside the scope of ATHOR Project.

As presented in this document, there are many techniques available for the evaluation of temperatures in industrial devices. However, the elevated temperatures in which refractory ceramics work may require some improvements, as these techniques may not be fully suitable. These improvements are being developed within the scope of WP1.

In conclusion, the improvement of measurement tools performed within WP1, including the "Tasks 1.1 - Thermal instrumentation", "Task 1.2 - Strain Instrumentation", "Task 1.3 – Devices for thermo-physical properties characterization" and "Task 1.4 - Devices for thermomechanical characterization" are increasing the current knowledge and will be used in "WP1 - Improvements of measurements tools", "WP2 - Advanced characterization of materials, refractories and joints" and "WP4 -Advanced measurements for numerical validation"

5. References

[1] J. Wu, "A Basic Guide to Thermocouple Measurements," *Texas Instruments*, no. September, pp. 1–37, 2018.

[2] P. Battalwar, J. Gokhale, and U. Bansod, "Infrared Thermography and IR Camera," *Int. J. Res. Sci. Eng.*, vol. 1, no. 3, pp. 9–14.

[3] E. Maeda, S. Terayama, M. Iida, and K. Nakai, "Author Guidelines for proceeding Evaluation of Rheological Properties of Tap-hole Materials," pp. 2–3.

[4] R. Lamm, S. Kirchhoff, and P. Technology, "Optimization of Ladle Refractory Lining , Gap and Crack Detection , Lining Surface Temperature and Sand-Filling of the Ladle-Taphole By Means of a 3D-Laserprofile-Measurement System That Is Immersed Into a Hot Ladle To Evaluate the Entire Condition," pp. 1–4.